ELECTRON CYCLOTRON RESONANCE ETCHING OF SILYLATED PHOTORESIST

by

Bob Lynch, Siddhartha Das, Michael A. Lieberman,
and Dennis W. Hess

Memorandum No. UCB/ERL M92/25

5 March 1992

ELECTRON CYCLOTRON RESONANCE ETCHING OF SILYLATED PHOTORESIST

by

Bob Lynch, Siddhartha Das, Michael A. Lieberman,
and Dennis W. Hess

Memorandum No. UCB/ERL M92/25

5 March 1992

ELECTRONICS RESEARCH LABORATORY

College of Engineering
University of California, Berkeley
94720

ELECTRON CYCLOTRON RESONANCE ETCHING OF SILYLATED PHOTORESIST

by

Bob Lynch, Siddhartha Das, Michael A. Lieberman,
and Dennis W. Hess

Memorandum No. UCB/ERL M92/25

5 March 1992

ELECTRONICS RESEARCH LABORATORY

College of Engineering
University of California, Berkeley
94720

ELECTRON CYCLOTRON RESONANCE ETCHING OF SILYLATED PHOTORESIST

Bob Lynch[1], Siddhartha Das[2], Michael A. Lieberman[3], and Dennis W. Hess[4]

[1]Department of Chemical Engineering
and
[3]Department of Electrical Engineering and Computer Science
University of California, Berkeley CA 94720

[2]Components Research, Intel Corporation, Santa Clara, CA 95052

[4]Department of Chemical Engineering
Lehigh University, Bethlehem, PA 18015

College of Engineering
University of California, Berkeley
94720

Abstract

The dry development of Plasmask 301-U resist was investigated using O_2 plasmas generated in an experimental electron cyclotron resonance reactor. An rf source operating at 13.5 MHz was used to independently bias the wafer holder. The dc component of the rf bias was used as a rough indication of the bombardment energy of ions incident on the wafer surface. The ECR plasma source was characterized using Langmuir probes and optical emission spectroscopy. Etch rates were measured as a function of reactor pressure, O_2 flow rate, wafer bias, and wafer distance from the ECR source chamber. Etch rates correlated most closely with ion current density over the range of variables studied. Etched profiles generated at different wafer positions, rf biasing conditions, oxygen gas flow rates, and gas pressures were investigated using scanning electron microscopy. The anisotropy of etched profiles improved with increasing rf bias and decreasing pressure. At very low oxygen flow rates, mask formation was inhibited; at high rf biases, mask sputtering was enhanced. Development of high resolution anisotropic profiles depended on a fine balance between silylation temperature, wafer bias, and etch pressure. Anisotropic, well-defined profiles of 0.30 μm lines and spaces were obtained at 0.5 mTorr and an applied bias of -60 volts.

I. Introduction

Surface imaging resist schemes including silylation methods show much promise in the development of sub-half micron lithography technologies. These schemes address the issues of topography, depth of focus, and reflectivity simultaneously. To date, much of the silylation research has focussed on the mechanisms of silylation[1,2,3], revealing the effects of photoactive compound (PAC) concentration, base resin composition, and silylation agents. Most silylated resists have been dry developed using reactive ion etch (RIE) sources or magnetically enhanced reactive ion etch (MERIE) sources[4]. Novel plasma sources, including electron cyclotron resonance (ECR)[5],

distributed ECR (DECR)[6], helicon sources[7], helical resonators[8], and other inductive sources[9], have demonstrated utility in semiconductor processing applications. Currently, few of these sources have been carefully investigated for etching silylated photoresist.

These novel plasma sources are reported to have relatively low incident ion energies, thus reducing the likelihood of silylated mask erosion or ion damage to the wafer during etching. Typically, RIE sources have ion energies in the 200-1000 eV range, while novel plasma sources have average ion energies around 20 eV. Moreover, ion energy at the wafer surface is controllable with many of the new sources by independently rf biasing the substrate. Using this approach, effects due to ion density and ion energy are decoupled, thus allowing better control of plasma etching.

In this study, we use an experimental ECR source to etch silylated photoresist. Atomic oxygen concentration, ion density, and ion energy are estimated using plasma diagnostics. These plasma parameters are then correlated with the observed etch rates and etch profiles.

II. Experimental

A. ECR System

The ECR plasma source used in this study is a modified version of a previous ECR source[10]. The system, displayed in Figure 1, consists of a source chamber and a processing chamber. Wafer samples are etched in the processing chamber at two positions. As shown in Figure 1, Positions 1 and 2 are respectively 29 cm and 14 cm from the edge of the source chamber. Gases fed into the source chamber are metered with MKS automatic flow controllers. The system is pumped by a CVC diffusion pump; pressure is maintained by a VAT automatic gate valve and pressure controller. A static magnetic field is superimposed on the ECR chamber by electromagnetic coils placed at each end of the source chamber and driven with 150 A dc current. Microwave power at 2.45 GHz cw is supplied through a WR284 waveguide and a 9.0 cm diameter quartz window into the source chamber.

Positive ions created in the ECR chamber bombard unbiased surfaces with low energies, typically 0-30 eV. Greater ion energies are achieved by rf biasing the wafer holder. In this study, a Wavetek signal generator and an ENI power amplifier were used to apply a 13.5 MHz bias to the wafer holder. The dc component of this applied bias was measured with a low pass filter. Ions with low mobility cannot respond to the high frequency field; rather, they are accelerated by the dc self bias of the 13.5 MHz field. In this ECR system, ions also gain energy due to the distributed electric field between the source and the processing chamber. However, this field is small, so that the energy gained in the sheath as indicated by the dc bias is a good first approximation of the total ion energy.

B. ECR Diagnostics

Plasma species, singly or in combination, are responsible for photoresist etching as well as silylated photoresist mask formation and sputtering. Cylindrical Langmuir probes were used to determine ion density as a function of position. Probes, made from 0.003" diameter tungsten wire, were inserted from the back of the chamber to yield axial information and from the side of the chamber, at Position 2, to yield radial profiles.

The wafer holders at Positions 1 and 2 were used as planar Langmuir probes to measure ion current densities. To achieve ion saturation with these planar probes, current to each wafer holder was limited by covering all but 1.26 cm^2 of each surface (in the center) with insulating glass.

Using optical emission spectroscopy (OES) and actinometry, relative bulk atomic oxygen concentration in the source chamber and at Position 2 was determined as a function of pressure. Due to a lack of optical access at Position 1, bulk atomic oxygen concentration could not be assessed at this location. Emission was measured with a PlasmaTherm Plasma-Scan system.

C. Wafer Processing

Wafers were coated with 1.0 μm of Plasmask 301-U DUV resist (UCB-JSR) and soft-baked at 100°C for 60 seconds. Patterns were exposed on a Nikon 248 nm laser stepper (NA=0.42, 5x reduction). Unless otherwise noted, wafers were silylated at 180°C. The wafers were first prebaked for 60 seconds in vacuum at the silylation temperature and then silylated for 60 seconds. Both presilylation bake and silylation were carried out in a Monarch 150 silylation oven. Silylation pressure was 50 Torr hexamethyldisilizane (HMDS).

Samples of roughly 5 cm^2 were used to maintain spatially uniform etch rates. Before etching, samples were thermally bonded, using Dow Corning 340 heat sink compound, to the center of the wafer holder. Wafer temperature during etching was monitored with a Luxtron fluoroptic thermometer. The fluoroptic probe contacted the back surface of wafer samples through a vacuum feedthrough on the back side of the Position 2 wafer holder.

Film thicknesses were measured with a NanoSpec/AFT interferometer. Etch rates of bulk unsilylated samples were determined by dividing the thickness loss by the etch time. Patterned silylated samples were etched for times calculated from the unsilylated sample etch rates and the desired percent overetch. No corrections were made for pattern dependent etch rate phenomena.

Etched profiles were investigated with a T-300 JEOL scanning electron microscope.

III. Results and Discussion

A. Plasma Characterization

Ion Density Estimates: Cylindrical Langmuir probe measurements yielded relative estimates of radial and axial ion density profiles. These profiles were produced at a microwave power of 500 Watts, an O_2 flow rate of 4.0 sccm, and a chamber pressure of 0.5 mTorr. Radial ion densities reached a maximum near the center of the chamber and decreased towards the walls. Such

nonuniform radial ion density profiles lead to nonuniform etch rates when etch behavior is ion current limited. The axial ion density increased exponentially from the back of the processing chamber into the source chamber 29 cm away. Typically, ion densities in the source chamber were greater than 10^{11} cm^{-3}. Since mean free paths for ion-neutral collisions at 0.5 mTorr are tens of centimeters, diffusion at this pressure was not an important transport mechanism. Rather, these ion density profiles were dictated by the plasma following the magnetic field line expansion from source chamber into processing chamber.

Ion Current Measurements: Ion current density at the center of each wafer holder was measured as a function of pressure. At Position 1, ion current peaked at 0.9 mA/cm^2 at about 0.5 mTorr, whereas, at Position 2, ion current peaked at 14 mA/cm^2 at approximately 1.0 mTorr. As pressure increased above these threshold values, ion current decreased due to diffusion to sidewalls, which lowered the current density measured along the centerline of the chamber.

Bulk Atomic Oxygen Concentration Estimates: The variation of atomic oxygen concentration with wafer bias and pressure was established using optical emission spectroscopy and actinometry. The 750.4 nm line was used to monitor Ar concentration and the 844.5 nm line was used to monitor atomic O concentration. Initially, emission was measured from a side window centered two centimeters in front of the wafer holder. No change in either Ar or O emission intensity was observed with increasing wafer bias. These data support our assumption that rf power applied to the wafer holder does not change the bulk plasma properties, but only increases the voltage drop across the normal sheath. Thus, any wafer bias dependency observed for material processing can be clearly attributed to ion energy effects alone.

Actinometry was used to determine the effect of pressure on the relative atomic oxygen concentration. The technique of actinometry[11] relies on an emission line from a trace gas to calibrate changes in signal intensity due to variations in either electron density or electron energy

distribution. In this study, Ar, used as the actinometer, was maintained at a constant partial pressure of 0.05 mTorr. The ratio of the O signal at 844.5 nm to the Ar signal at 750.4 nm yielded a relative measure of the atomic O concentration. In the source chamber, O concentration varied with pressure as shown in Figure 2. At low pressures, O concentration increased linearly with pressure. After a short transition region, O concentration saturated at a pressure of about 4 mTorr.

Wafer Temperature: For high bias experiments (-100 V) at Position 2, the temperature of thermally bonded wafer samples sometimes approached 100°C, but for all other experiments, maximum wafer temperature never exceeded 60°C. Wafer temperature at Position 1 was not measured; however, lower maximum temperatures at this location were assured since the ion current density (the main heating source[12]) at Position 1 was more than an order of magnitude less than at Position 2.

B. Etch Rates

Unless otherwise noted, all samples were etched at 1.0 mTorr, 4.0 sccm O_2, 500 W microwave power, and -20 V bias voltage. The etch rate data for unsilylated samples are consistent with a model[13] based on the reaction of photoresist with adsorbed atomic O, followed by ion-induced desorption of the etch products. In such a model, etching is rate limited by the depleted specie, either ions or atomic O.

In Figure 3, etch rate is plotted versus pressure for samples etched at Positions 1 and 2. The etch rate reached a maximum value at a pressure which depended on the wafer holder position. At Position 2, the maximum etch rate of 0.9 μm/min occurred at about 1.0 mTorr, while at Position 1, the maximum etch rate of 0.2 μm/min occurred at a pressure of approximately 0.5 mTorr. At both positions, the etch rates peaked at the same pressure as did the ion current density. With increasing pressure, the etch rate decreased, again similar to the ion current density behavior. These trends

suggest that at an O_2 flow rate of 4.0 sccm and 500 Watts microwave power, atomic O is in excess and etching is controlled by ion current density. Etch rates at Position 1 were more reproducible (see Figure 3) than those at Position 2 due to the averaging of processing transients over the longer etch times required at Position 1.

The etch rate increased and then saturated with increasing O_2 flow rate, as illustrated in Figure 4. Saturation occurred at 3-4 sccm O_2 at an etch rate of about 0.2 μm/min. In the unsaturated region, the etch rate was limited by atomic O concentration. In the saturated region, etch rate was limited by ion current density, which did not change appreciably with O_2 flow rate. Similar etch rate behavior in other ECR sources has been reported previously[5,13].

The effect of wafer bias on etch rate is shown in Figure 5. In this experiment, plasma ion density and neutral concentrations remained constant. Samples were etched at Position 1, using 500 Watts microwave power and an O_2 flow rate of 4.0 sccm. When the dc wafer bias was increased from -20 V to -80 V, etch rates at both 1.0 and 5.0 mTorr roughly doubled. This dependency of etch rate on ion energy is further indication that photoresist etching is ion assisted. Heidenreich et al[14] noted similar behavior for polyimide and photoresist etching; they suggested the creation of reactive sites, breaking of chemical bonds, and the generation of heat at the photoresist surface as etch mechanisms which depend on ion bombardment energy.

C. Etched Profiles

Scanning electron micrographs (SEMs) were used to investigate the effect of plasma conditions on etched profiles. Most samples were overetched by at least 20% according to etch rates determined for bulk unsilylated samples. However, the etch rate of unexposed photoresist was slower for silylated samples than for unsilylated samples. This effect was caused by silicon uptake in the unexposed regions (described below). As a result, photoresist material remained in the etched

trenches of many of the profiles shown in the following figures. These remaining regions of photoresist were generally less than 10% of the thickness of the protected photoresist layer and thus did not compromise the analysis of the etched profiles. Microwave power was set at 500 W for all etched samples. Profiles shown are ostensibly of 0.50 μm equal lines and spaces, unless otherwise noted.

Wafer Bias and Reactor Pressure: The effect of wafer bias and ECR reactor pressure on etched profiles is described using Figures 6-11. These profiles are from samples silylated at 180°C and etched at Position 1, using 4.0 sccm O_2. All samples were overetched by 20% which, upon SEM analysis, was found to be insufficient for complete photoresist removal. Pressures of 0.5, 1.0, and 5.0 mTorr, and wafer biases of -20 and -60 V were investigated. As demonstrated in Figures 6, 8, and 10, anisotropy changed significantly with pressure at a wafer bias of -20 V. As pressure increased at this bias, the degree of anisotropy decreased. An extreme case is the sample etched at 5.0 mTorr and -20 V (Figure 10), where lateral etching is pronounced. This decrease in anisotropy with increasing pressure is partly due to the decreasing vertical etch rate (dictating longer plasma exposure), and partly to sidewall surface bombardment by ions with energy components parallel to the sample surface. Such ions result from ion-neutral collisions in the sheath.

An increase in wafer bias was used to further enhance ion energy perpendicular to the wafer surface, thus increasing the vertical etch rate and reducing the ion scattering effect due to sheath collisions. With samples etched at -60 V bias (Figures 7, 9, and 11), anisotropy was less affected by changes in pressure. At this bias and 0.5 mTorr pressure, anisotropic profiles of 0.3 μm lines and spaces, as shown in Figure 12, were etched from samples silylated at 170°C. The effect of wafer bias on profile anisotropy was most apparent at high pressure, as illustrated in Figures 10 and 11. For the profile etched with -60 V bias (Figure 11), lateral etching was significantly less than for the profile etched with -20 V bias (Figure 10).

Incomplete removal of photoresist (see Figures 6-11) after overetching by 20% motivated an experiment in which samples were overetched by 40% using the same conditions as above. With this longer overetch, profiles demonstrated complete photoresist removal. An example is the profile etched at 0.5 mTorr and -60 V bias, shown in Figure 13.

A second set of samples was etched at Position 2, using the same silylation and etching conditions as those used for the profiles etched at Position 1. This second set of profiles showed similar behavior to those etched at Position 1. At -20 V bias, anisotropy worsened markedly as pressure increased from 0.5 mTorr to 5.0 mTorr. At -60 V bias, profiles displayed excellent anisotropy, roughly independent of pressure. One important difference between profiles etched at the two positions was that silylation masks of samples etched at Position 2 formed more completely than those of samples etched at Position 1. Mask formation, believed to result from the reaction between incorporated silicon and plasma generated atomic O, was more complete at Position 2 because of the higher atomic O concentration at that location. Ion current density, also much higher at Position 2 than at Position 1, increased ion sputtering of mask material. However, at -20 and -60 V wafer bias, the elevated sputtering rate did not compensate for the enhanced mask formation, perhaps because the high etch rates at Position 2 led to shorter etch times and thus less time for sputtering. Indeed, significant photoresist remained even after 40% overetch, suggesting the presence of silicon and thus partial mask formation in nominally unexposed (therefore unsilylated) regions.

Silylation Temperature: Incomplete removal of photoresist from nominally unexposed regions became more severe as line widths decreased below 0.50 μm, regardless of wafer position. To determine whether this effect was in fact due to mask formation in nominally unsilylated regions rather than microloading, silylation temperature was varied to change the overall amount of silicon incorporation. Figures 14-17 are used to compare the effect of silylation temperature on etched profiles. The profiles in Figures 14 and 16 are from samples silylated at 170°C, while the profiles

in Figures 15 and 17 are from samples silylated at the 180°C. In this experiment, all samples were etched at Position 1 at 0.5 mTorr, using 4.0 sccm O_2 and -60 V wafer bias. Etched profiles from samples silylated at 170°C displayed complete etching in unsilylated regions, regardless of line width. For the samples silylated at 180°C, only the etched profile of 0.40 μm lines (Figure 17) displayed complete etching. Less photoresist was removed from the profile of 0.30 μm lines (Figure 15), and very little photoresist was removed from the profile of 0.25 μm lines (not shown). Since etch rate was independent of line width for samples silylated at 170°C, microloading, which is independent of silylation, cannot explain the pattern dependent etch rate observed for samples silylated at 180°C. Rather, this effect was caused by silicon incorporation in ostensibly unexposed, unsilylated regions. The effect occurred only for samples silylated at 180°C because of the greater amount of silicon incorporated at this temperature. The substantial difference in the profiles shown in Figures 14 and 15 demonstrates the unusual sensitivity of ECR plasma etched profiles on silylation temperature. Unfortunately, this advantage of silylating wafers at 170°C to realize pattern independent etch rates was accompanied by a critical dimension loss of etched lines.

Silylation Mask Integrity: Etched profiles were used to examine the integrity of silylated masks at low O_2 flow rates and at high wafer bias. The formation step, dependent on atomic oxygen concentration, was investigated by decreasing the O_2 flow rate, which lowered the relative atomic O concentration as measured by optical emission spectroscopy. Wafers were etched at Position 1 at 0.5 mTorr, using -60 V applied bias. At the standard O_2 flow rate of 4.0 sccm, silylated masks formed and remained stable during plasma etching. At 1.0 sccm O_2 flow rate, the pattern shown in Figure 18 was delineated. This pattern resembles patterns etched at the standard flow rate of 4.0 sccm O_2, illustrating the presence of sufficient atomic O in the plasma for complete mask formation. However, at 0.5 sccm O_2 flow rate, the tapered profile in Figure 19 demonstrated incomplete mask formation due to insufficient atomic O concentration in the plasma. The tapered shape resulted from decreased

protection at the edges of each line due to the convex lens shape of the organosilicon layer. At 0.1 sccm O_2 flow rate, no profiled pattern remained upon complete etching, indicating little or no integral mask formation. Further experiments demonstrated that the flow rate threshold for proper mask formation changed depending on silylation temperature and substrate bias.

Even with an atomic O concentration adequate for suitable mask generation, poor mask integrity can result. Such is the case for samples subjected to surface bombardment by high energy ions. This effect was studied at a wafer bias of -100 V and pressures of 0.5, 1.0, and 5.0 mTorr. In this experiment, samples were etched at Position 2 and an O_2 flow rate of 4.0 sccm. No pattern remained upon completion of the 0.5 mTorr etch, while profiles etched at 1.0 and 5.0 mTorr are shown in Figures 20 and 21 respectively. As with the tapered profile shown in Figure 19 and discussed in the preceding paragraph, the tapered profile displayed in Figure 20 is also an artifact of imperfect protection of the convex lens shaped organosilicon layer. The improvement in mask integrity as pressure increased is attributed to two causes. First, atomic O concentration increased as pressure increased (see Figure 3), resulting in better mask formation. Second, with increasing pressure, ion current density decreased, thus lowering the sputtering rate of mask material. The combination of these two phenomena resulted in complete mask integrity for the 5.0 mTorr etch, poor mask integrity for the 1.0 mTorr etch, and no mask integrity for the 0.5 mTorr etch.

Wafer Temperature: The need to thermally bond wafers to a heat sink was demonstrated by etching a sample with no thermal grease between the sample and the substrate. At Position 2, with a -60 V bias etch at 0.5 mTorr, the wafer temperature rose by more than 250°C in 63 seconds. The temperature history of this sample is shown in Figure 22, and the etched profile of 0.50 μm lines is demonstrated in Figure 23. Clearly, flow deformation of the Plasmask photoresist occurred.

Residue: No residue (grass) was observed in any of the profiles etched in this ECR reactor. This result is not apparent in some figures due to incomplete etching of the photoresist. However,

in figures in which the photoresist was etched to completion, eg. Figures 14 and 21, no residue was discerned on the bare silicon substrate.

IV. Conclusions

ECR etching of silylated Plasmask 301-U photoresist has been demonstrated. At low wafer bias, anisotropy improved as pressure decreased. Anisotropy also improved at high wafer bias. Mask integrity exhibited extreme sensitivity to silylation temperature, resulting in poor mask protection at low silylation temperatures and silicon incorporation into unexposed areas at high silylation temperatures. Mask integrity also diminished at low flow rates and high bias conditions. The balance between an appropriate silylation temperature and wafer bias was delicate. Furthermore, the need for heat removal from wafer samples was established. No residue was observed for profiles etched completely to the silicon substrate. Well-defined anisotropic profiles of 0.30 μm lines were obtained at 0.5 mTorr and -60 V bias.

V. Acknowledgements

This work was supported by Sematech SRC Grant #91-MC-500 and Department of Energy Grant #DE-FG03-87ER13727. Bob Lynch gratefully acknowledges Arthur Sato and Robert Porteous for helpful discussions on ECR and other plasma sources. Siddhartha Das acknowledges Henry Gaw for project support, Chien Chiang for useful discussion, and Izabell Guderski for SEM support.

References

1. B. Roland, R. Lombaerts, J. Vandendriessche, and F. Godts, *Proceedings SPIE*, Vol. 1262, pp. 151-160 (1990) and references therein.

2. R.J. Visser, J.P.W. Schellekens, M.E. Reuhman-Huisken, and L.J. Van Ijzendoorn, *Proceedings SPIE*, Vol. 771, pp. 111-118 (1987).

3. T.T. Dao, C.A. Spence, D.W. Hess, *Proceedings SPIE*, Vol. 1466, pp. 257-268 (1991).

4. C.M. Garza, D.L. Catlett, and R.A. Jackson, *Proceedings SPIE*, Vol 1466, pp. 616-628 (1991).

5. J. Forster and W. Holber, *J. Vac. Sci. and Technol.*, A 7(3), pp. 889-902, (1989).

6. J. Dijkstra, G. van de Ven, H. Kalter, *Microelectronic Engineering*, 13, pp. 455-461 (1991).

7. A.J. Perry, D. Vender, and R.W. Boswell, *J. Vac. Sci. and Technol.*, B 9(2), pp. 310-317 (1991).

8. J.M. Cook, D.E Ibbotson, P.D. Foo, and D.L Flamm, *J. Vac. Sci. and Technol.* A 8(3), pp. 1820-1824 (1990).

9. J.A. Hopwood, C.R. Guarnieri, S.J. Whitehair, and J.J Cuomo, presented at the AVS 38th National Symposium, Plasma Science Division; Seattle, Washington (1991).

10. D.A. Carl, D.W. Hess, and M.A. Lieberman, *J. Vac. Sci. and Technol.*, A 8(3), pp. 2924-2930 (1990).

11. J.W. Coburn and M. Chen, *J. Appl. Phys.*, 51(6), pp. 3134-3136 (1980).

12. A. Durandet, O. Joubert, and J. Pelletier, *J. Appl. Phys.*, 67(8), pp. 3862-3866 (1990).

13. O. Joubert, J. Pelletier, and Y. Arnal, *J. Appl. Phys.*, 65(12), pp. 5096-5100 (1989).

14. J.E. Heidenreich, J.R. Paraszczak, M. Moisan, and G. Sauve, *Microelectronic Engineering*, 5, pp. 363-374 (1986).

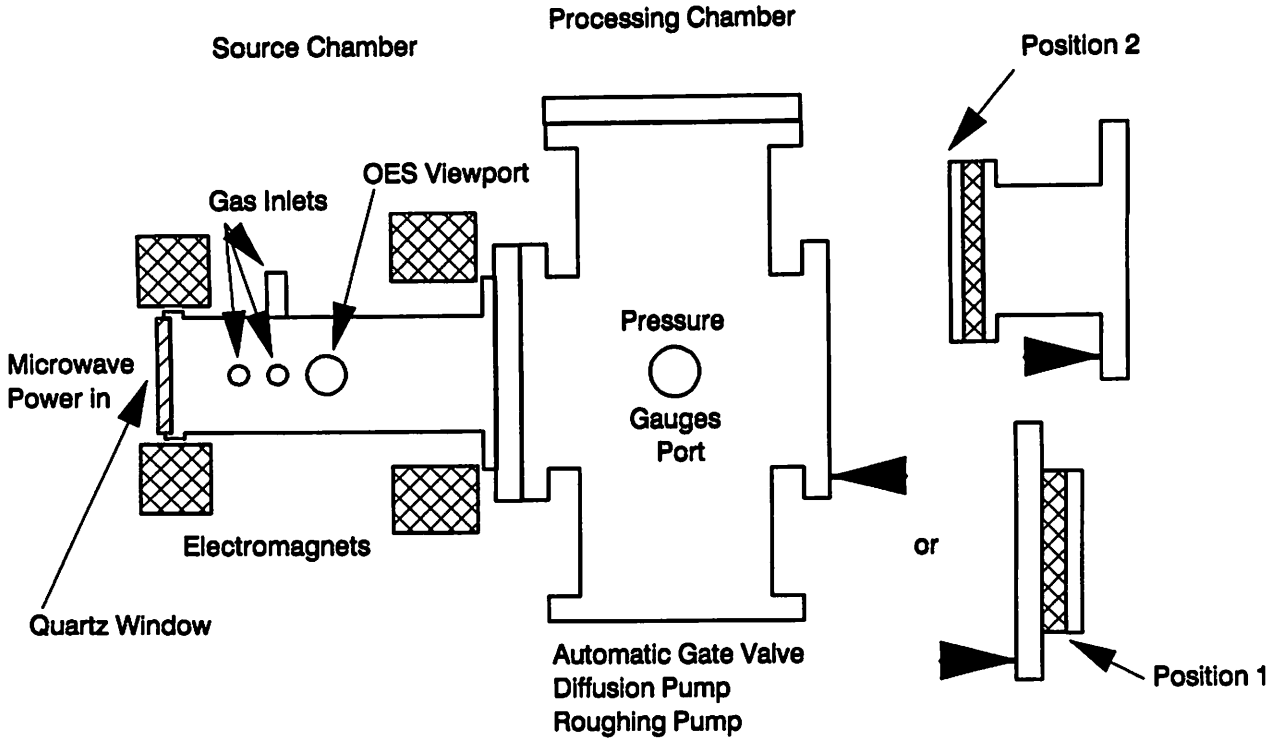

Figure 1. ECR system consisting of source chamber, processing chamber, and two wafer holders.

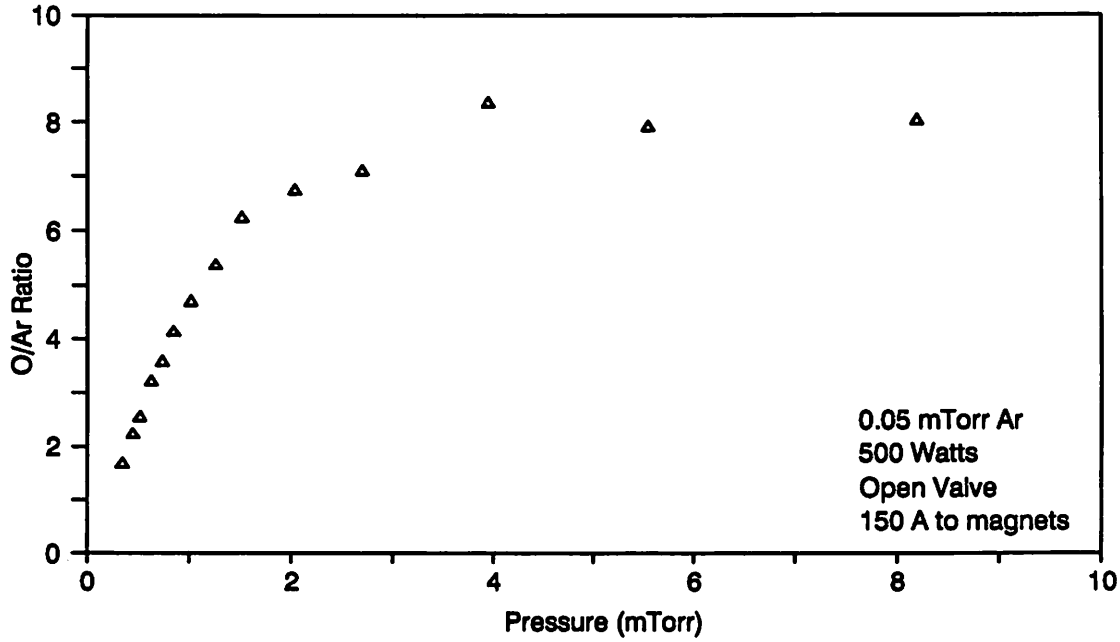

Figure 2. O/Ar signal ratio in the source chamber versus pressure (mTorr).

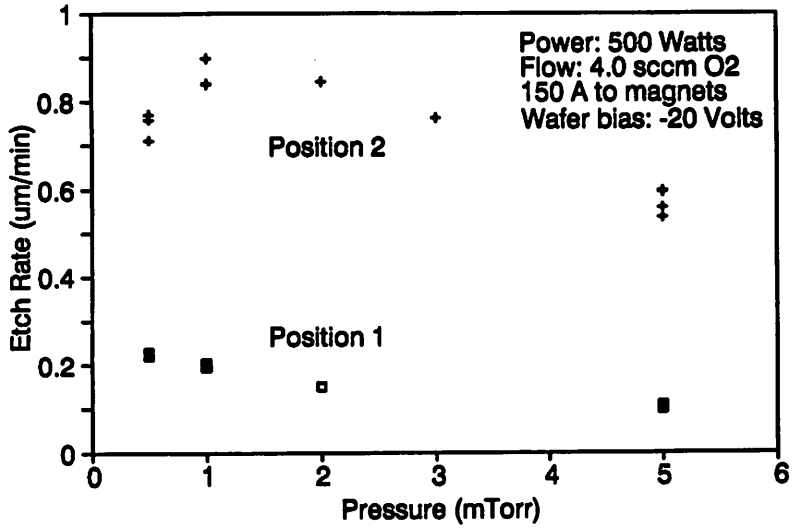

Figure 3. Etch Rate (μm/min) versus pressure (mTorr) at Positions 1 and 2

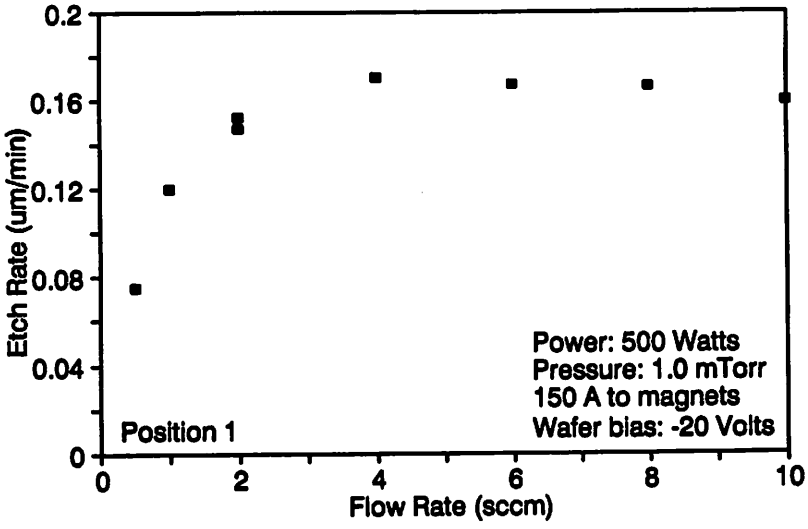

Figure 4. Etch Rate (μm/min) versus O_2 flow rate (sccm) at Position 1

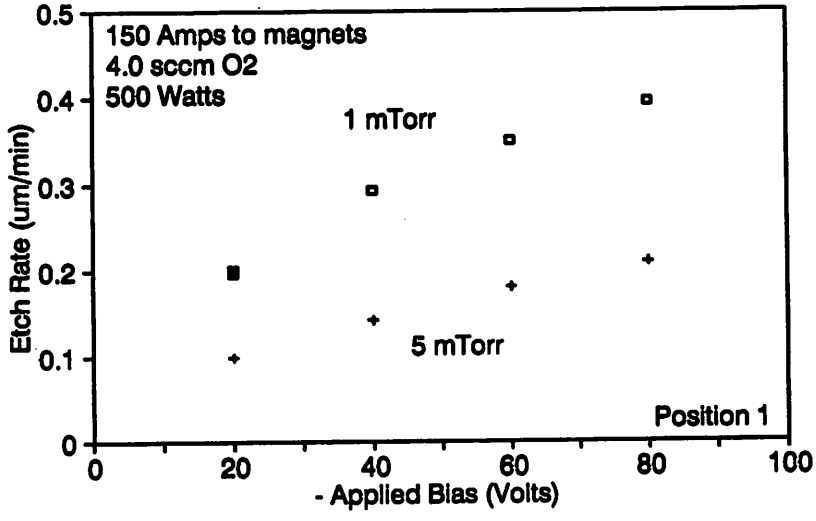

Figure 5. Etch Rate (μm/min) versus wafer bias (Volts) at 1.0 and 5.0 mTorr - Position 1

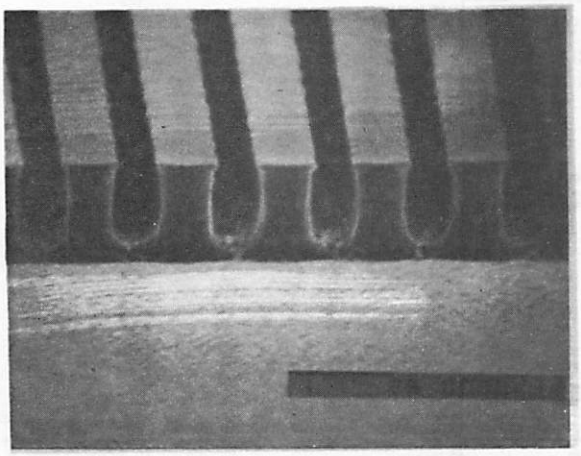

Figure 6. Etched @ 0.5 mT, -20 V wafer bias

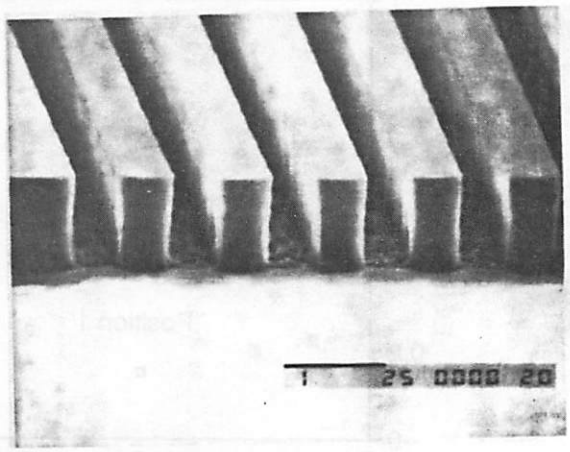

Figure 7. Etched @ 0.5 mT, -60 V wafer bias

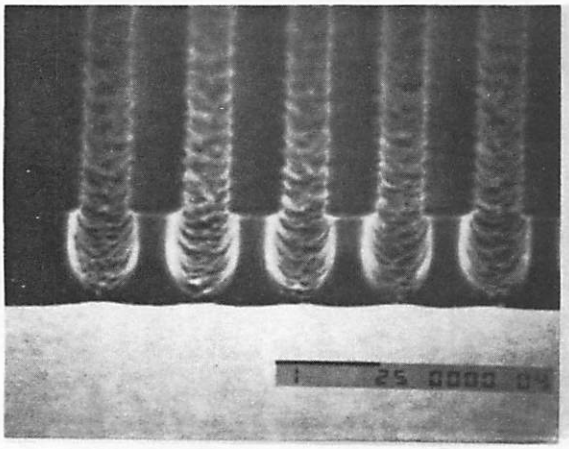

Figure 8. Etched @ 1.0 mT, -20 V wafer bias

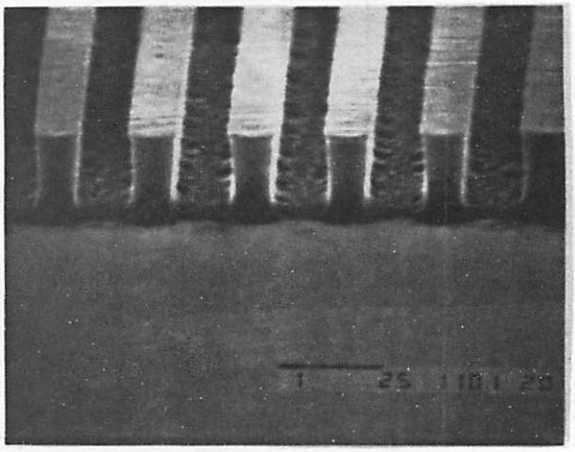

Figure 9. Etched @ 1.0 mT, -60 V wafer bias

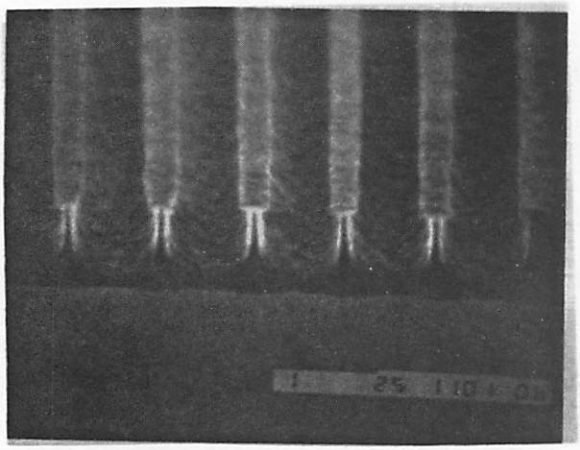

Figure 10. Etched @ 5.0 mT, -20 V wafer bias

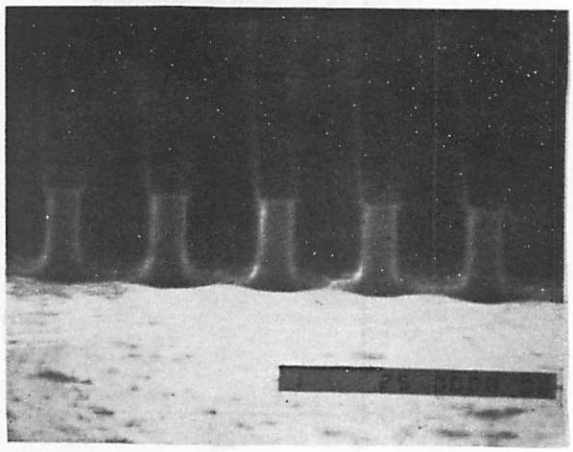

Figure 11. Etched @ 5.0 mT, -60 V wafer bias

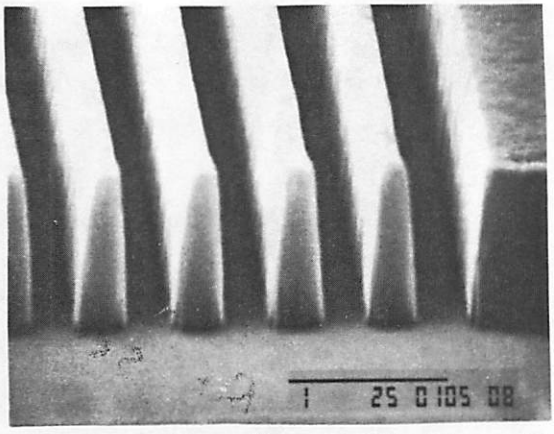

Figure 12. 0.30 μm lines @ 0.5 mTorr, -60 V

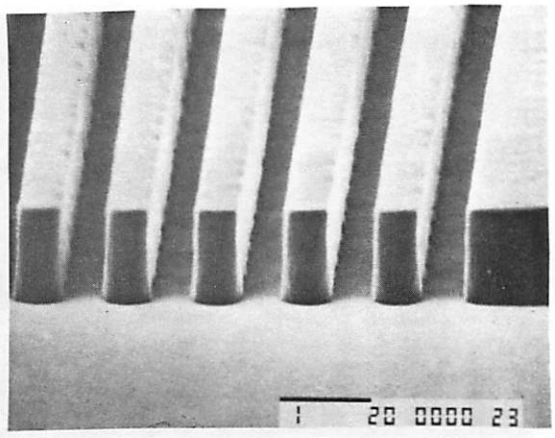

Figure 13. 40% overetch → clean Si substrate

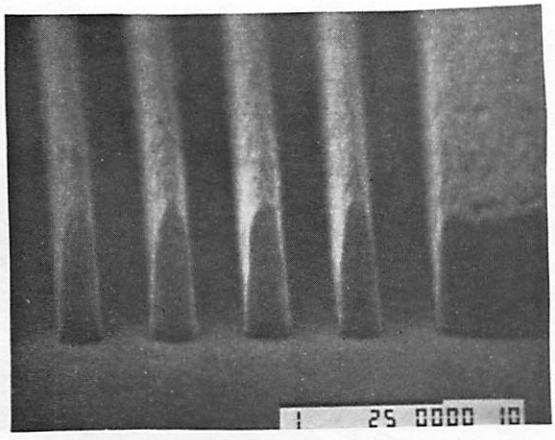

Figure 14. Silylated @ 170°C, 0.30 μm lines

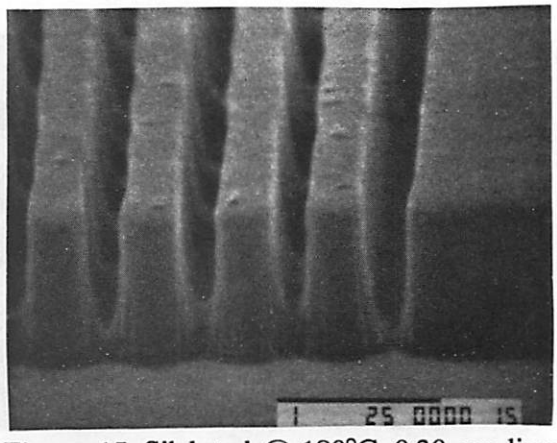

Figure 15. Silylated @ 180°C, 0.30 μm lines

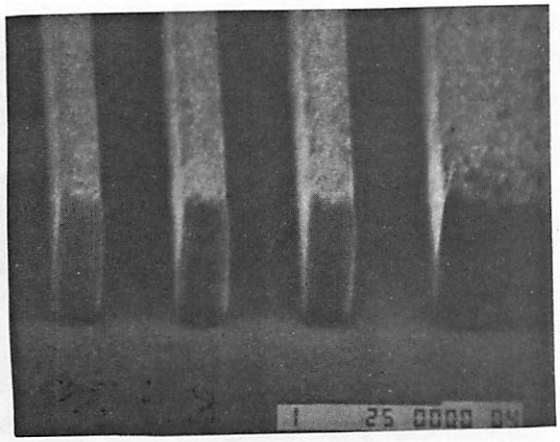

Figure 16. Silylated @ 170°C, 0.40 μm lines

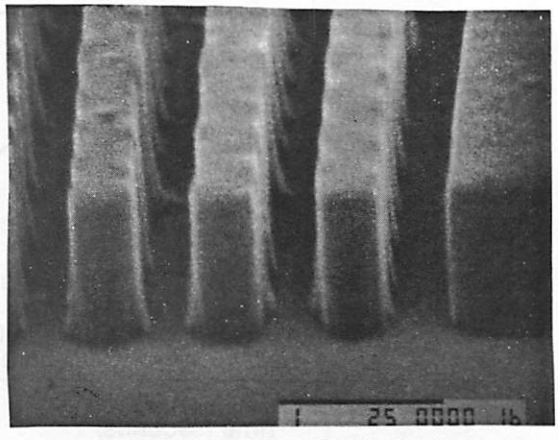

Figure 17. Silylated @ 180°C, 0.40 μm lines

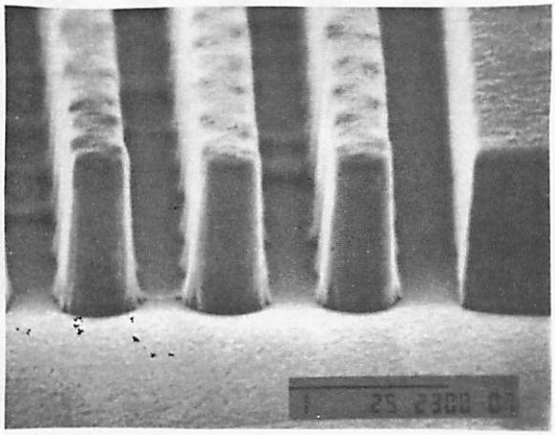

Figure 18. Etched @ 1.0 sccm O_2 flow rate

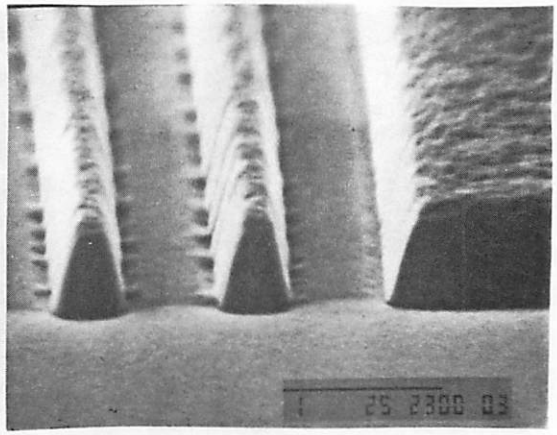

Figure 19. Etched @ 0.5 sccm O_2 flow rate

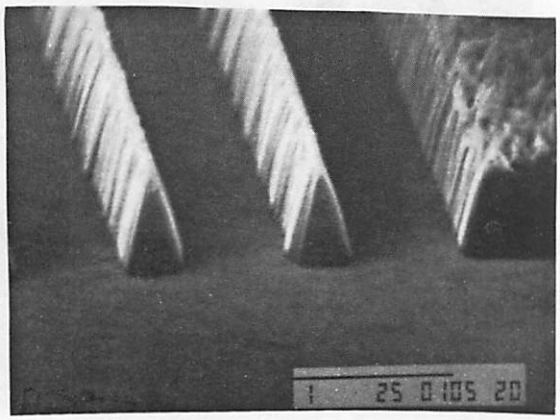

Figure 20. Etched @ 1.0 mTorr, -100 V bias

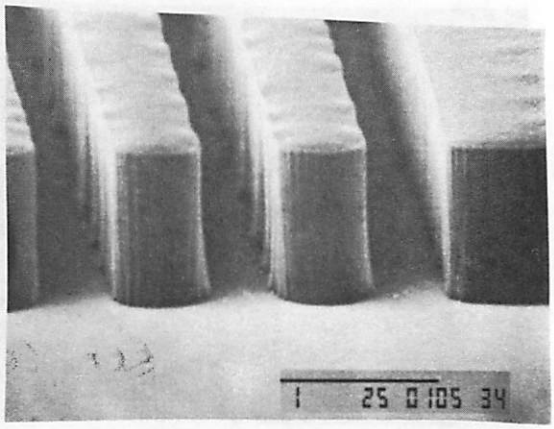

Figure 21. Etched @ 5.0 mTorr, -100 V bias

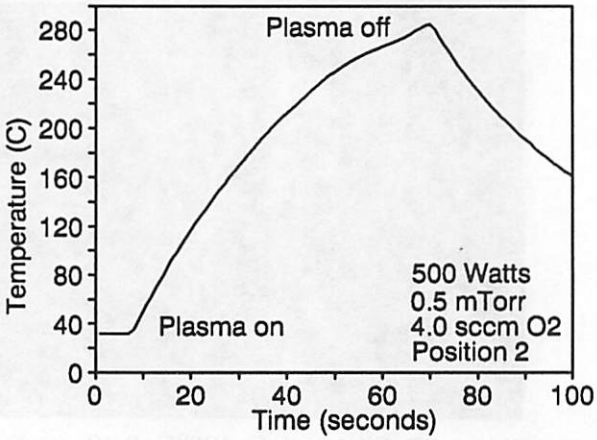

Figure 22. Temperature history of unbonded sample

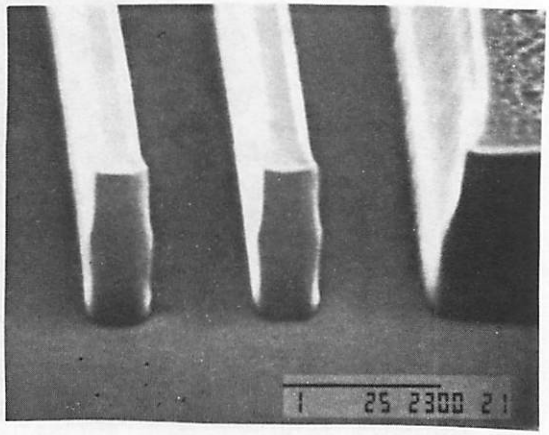

Figure 23. Etched profile of unbonded sample